ACS OMEGA

http://pubs.acs.org/journal/acsodf

Article

Application of Nanomagnetic Metal−Organic Frameworks in the Green Synthesis of Nicotinonitriles via Cooperative Vinylogous Anomeric-Based Oxidation

Bashirullah Danishyar, Hassan Sepehrmansourie, Hossein Ahmadi, Mahmoud Zarei,* Mohammad Ali Zolfigol,* and Mojtaba Hosseinifard

Cite This: *ACS Omega* 2023, 8, 18479−18490

Read Online

ACCESS | Metrics & More | Article Recommendations | Supporting Information

ABSTRACT: In the current study, we synthesized a new nanomagnetic metal−organic framework Fe_3O_4@MIL-53(Al)-N$(CH_2PO_3)_2$ and characterized it using various techniques. This nanomagnetic metal−organic framework was used for the synthesis of a wide range of nicotinonitrile derivatives as suitable drug candidates by a four-component reaction of 3-oxo-3-phenylpropanenitrile or 3-(4-chlorophenyl)-3-oxopropanenitrile, ammonium acetate (NH_4OAc), acetophenone derivatives, and various aldehydes including those bearing electron-donating, electron-withdrawing, and halogen groups, which afforded desired products (27 samples) via a cooperative vinylogous anomeric-based oxidation (CVABO) mechanism under solvent-free conditions in excellent yields (68−90%) and short reaction times (40−60 min). Increasing the surface-to-volume ratio, easy separation of the catalyst using an external magnet, and high chemical and temperature stability are the advantages of the described nanomagnetic metal−organic frameworks.

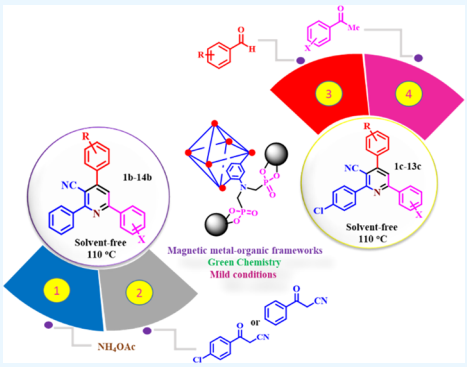

INTRODUCTION

Nowadays, a new class of porous materials has been developed by linking metal ions with organic compounds as ligands. This class of porous compounds grown in 3D space constitute metal−organic frameworks (MOFs).[1−3] By selecting the appropriate metal, ligand, and reaction conditions, the particle size, pore structure, and morphology can be designed and adjusted.[4,5] Metal−organic frameworks (MOFs) as multivariate materials have been widely used in drug delivery, biotechnology, magnetic resonance imaging (MRI), adsorption and desorption, gas separation, catalysis, and photocatalysis.[6−10] Despite many applications, nanomagnetic particles (Fe_3O_4) are used as suitable cores in catalysts.[11] The high stability and high surface-to-volume ratio will lead to an amazing integration between nanomagnetic materials and metal−organic frameworks (MOFs). According to the above-mentioned facts, nanomagnetic metal−organic frameworks are easily separated from the reaction by an external magnetic field.[12] Furthermore, the advantage of heterogeneous catalysts over homogeneous ones is their easy separation and recovery in organic reactions.[13,14] Many methods have been reported for the synthesis of nanomagnetic metal−organic frameworks as heterogeneous catalysts.[15−17] Recently, we introduced metal−organic frameworks and other molecules with phosphorous acid pendent groups (N-C-$(PO_3H_2)_2$),[18−20] melamine,[21] glycoluril,[22] carbon quantum dots (CQDs),[23] and mesoporous materials (SBA-15)[24] as novel heterogeneous catalysts in the preparation of biologically active organic compounds.

In recent research, *N*-heterocyclic compounds such as nicotinonitriles or triaryl pyridines have been considered for the preparation of various biologically active compounds with antiviral, antibacterial, anticonvulsant, and antioxidant properties, which are also useful in the treatment of breast and lung cancer (Figure 1).[25−27] Furthermore, changing substitutions at various ring positions of pyridine can also enhance the biological activities of nicotinonitriles.[28,29] Therefore, research and development are necessary and important in the synthesis of new compounds with *N*-scaffold compounds.

In the past, J.T. Edward introduced the anomeric effect (AE) concept to explain the chemical stability and mechanism in organic synthesis.[30] When sharing of electrons occurs through double bonds, it is called the vinylogous anomeric effect (VAE).[31,32] Although different kinds of anomeric effects have been reported in the literature, in this study, cooperative VAE is our main interest (Scheme S1). Recently, we reviewed the influence of AE in chemical processes.[33,34] Also, we introduced

Received: December 31, 2022
Accepted: April 24, 2023
Published: May 17, 2023

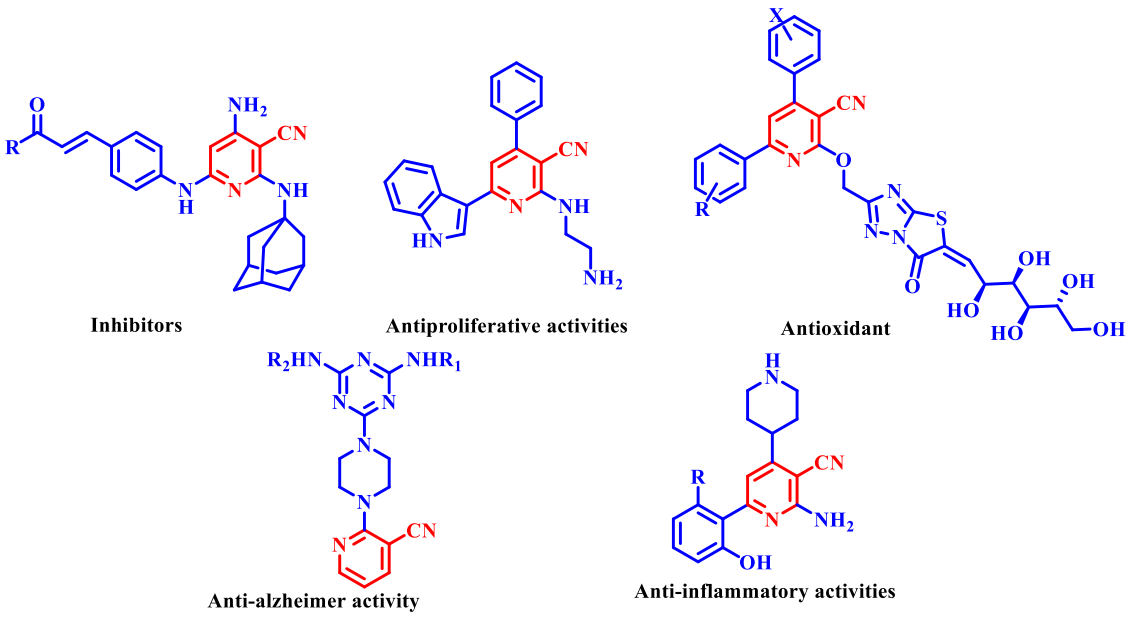

Figure 1. Structure of medicinal compounds containing nicotinonitrile.

Scheme 1. Preparation of Nicotinonitriles Using Fe_3O_4@MIL-53(Al)-N(CH_2PO_3)$_2$ as the Nanomagnetic Metal−Organic Framework

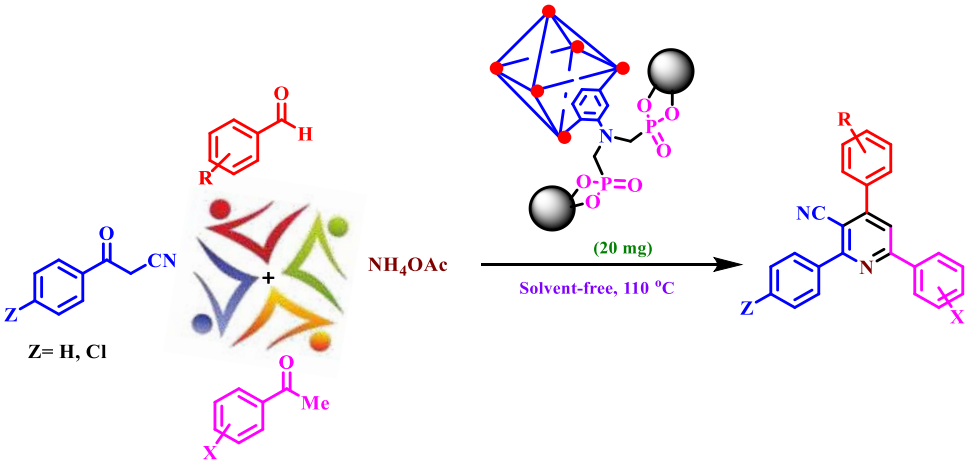

the concept of anomeric-based oxidation (ABO) as a driving force in the synthesis of susceptible molecules.[35,36] Besides, this concept has been presented in the oxidation and/or reduction of $NADP^+$/NADPH or NAD^+/NADH systems via hydride transfer.[37] The development of the cooperative vinylogous anomeric-based oxidation (CVABO) concept is our research interest.

Based on the feature mentioned herein, we wish to synthesize novel nicotinonitrile derivatives via the condensation of 3-oxo-3-phenylpropanenitrile or 3-(4-chlorophenyl)-3-oxopropanenitrile, aldehyde, acetophenones, and ammonium acetate using Fe_3O_4@MIL-53(Al)-N(CH_2PO_3)$_2$ as a nanomagnetic and porous catalyst (Scheme 1).

EXPERIMENTAL SECTION

Preparation of Nanomagnetic Metal−Organic Frameworks Based on Al. According to the previously reported literature, MIL-53(Al)-NH_2 and MIL-53(Al)-N($CH_2PO_3H_2$)$_2$ were synthesized.[20] Then, in a 50 mL round-bottomed flask, a mixture of MIL-53(Al)-N($CH_2PO_3H_2$)$_2$ (0.65 g) and Fe_3O_4 (0.5 g) was stirred in toluene (15 mL) as a solvent at 80 °C for 12 h. After cooling the reaction mixture, the composite was separated by an external magnet. Finally, the pure Fe_3O_4@MIL-53(Al)-N(CH_2PO_3)$_2$ was washed with ethanol (3 × 10 mL) and collected using an external magnet (Scheme 2).

General Procedure for the Preparation of Nicotinonitrile Derivatives. According to the previously reported procedure, 3-oxo-3-phenylpropanenitrile and 3-(4-chlorophenyl)-3-oxopropanenitrile were prepared as starting materials (Scheme 3).[38] In a 20 mL round-bottomed flask, a mixture of starting materials (1 mmol), aldehydes (1 mmol), acetophenones (1 mmol), ammonium acetate (1.5 mmol, 0.115 g), and Fe_3O_4@MIL-53(Al)-N(CH_2PO_3)$_2$ (20 mg) were stirred at 110 °C in solvent-free conditions. The progress of the reaction was followed by the TLC technique (*n*-hexane/ethyl acetate 1:1). After the completion of the reaction, the catalyst was separated from the reaction mixture by adding hot ethanol (20 mL) and using an external magnet. The precipitate was cooled and dried after filtration. The pure product was obtained by washing several times with ethanol (Scheme 1).

https://doi.org/10.1021/acsomega.2c06651
ACS Omega 2023, 8, 18479−18490

Scheme 2. Preparation of Fe_3O_4@MIL-53(Al)-N(CH_2PO_3)$_2$

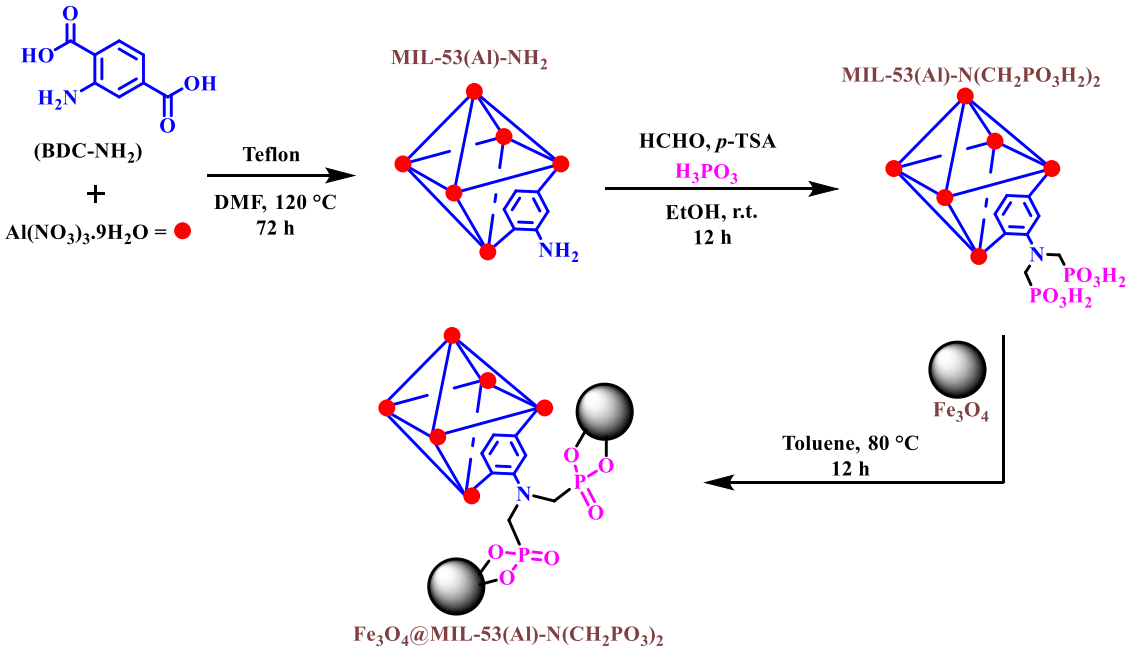

Scheme 3. Preparation of 3-Oxo-3-phenylpropanenitrile and 3-(4-Chlorophenyl)-3-oxopropanenitrile

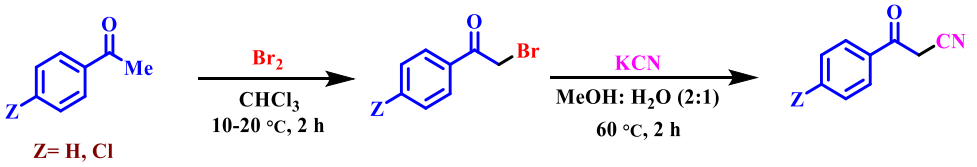

RESULTS AND DISCUSSION

Al-based metal−organic framework catalysts functionalized with phosphorous acid have been previously reported by our research group.[20] In a previous report, the metal−organic framework MIL-53(Al)-NH_2 was synthesized using an electrochemical method. By applying various analyses, its structure was well established, and the obtained results were in good agreement with previously reported methods. Linking phosphorous acid tags with the prepared Al-based MOFs produced its corresponding post-modified form MIL-53(Al)-N($CH_2PO_3H_2$)$_2$ as a porous acidic catalyst. Subsequently, the magnetic properties of Fe_3O_4 were used to create a new magnetic catalyst. By combining Al-based metal−organic frameworks functionalized with phosphorous acid and Fe_3O_4, we synthesized a novel nanomagnetic metal−organic frame-

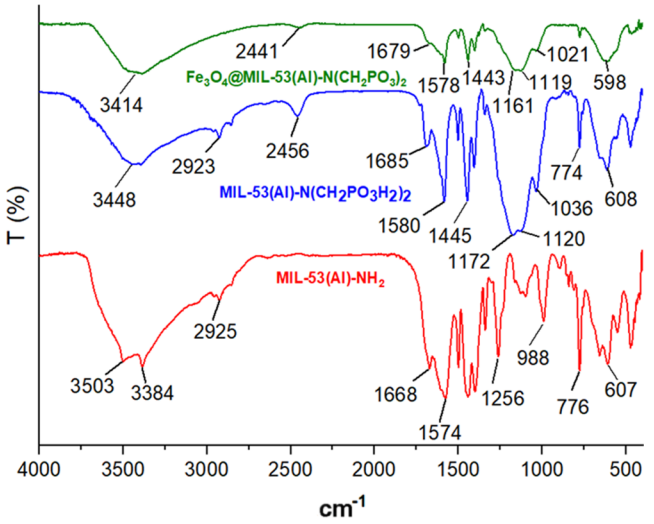

Figure 2. FT-IR spectra of MIL-53(Al)-NH_2, MIL-53(Al)-N-($CH_2PO_3H_2$)$_2$, and Fe_3O_4@MIL-53(Al)-N(CH_2PO_3)$_2$.

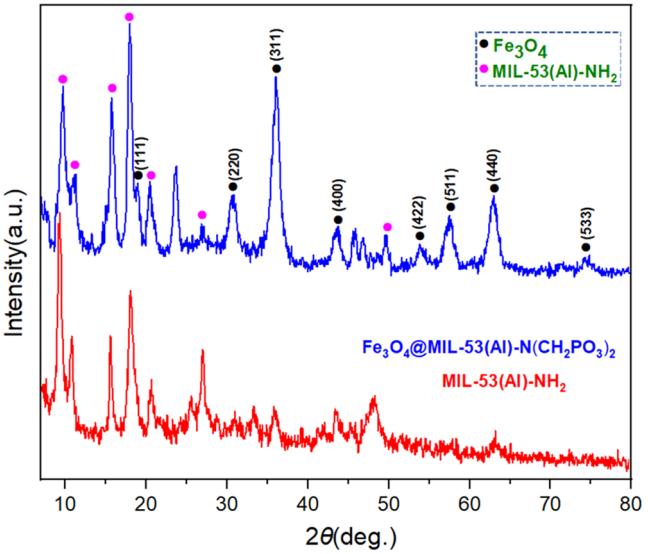

Figure 3. XRD patterns of MIL-53(Al)-NH_2 and Fe_3O_4@MIL-53(Al)-N(CH_2PO_3)$_2$.

https://doi.org/10.1021/acsomega.2c06651
ACS Omega 2023, 8, 18479−18490

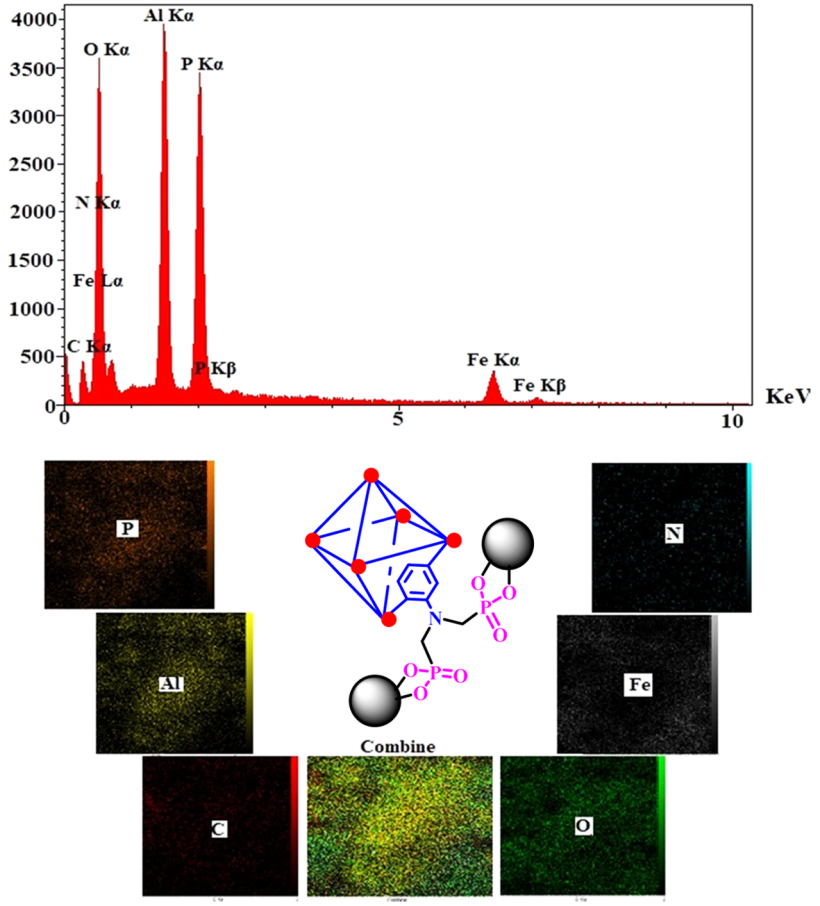

Figure 4. Energy-dispersive X-ray (EDX) analysis and elemental mapping of C (red), N (blue), O (green), Al (yellow), Fe (gray), and P (orange) atoms for Fe_3O_4@MIL-53(Al)-N(CH_2PO_3)$_2$.

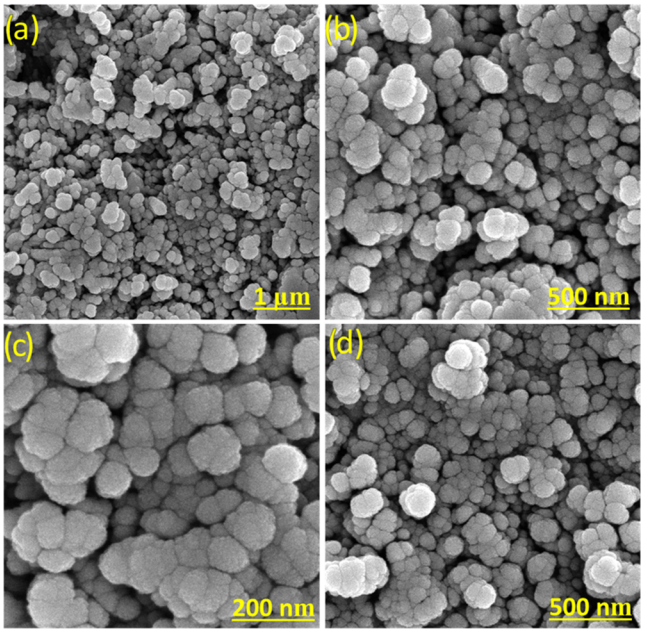

Figure 5. SEM images of (a, b) MIL-53(Al)-NH_2 and (c, d) Fe_3O_4@MIL-53(Al)-N(CH_2PO_3)$_2$.

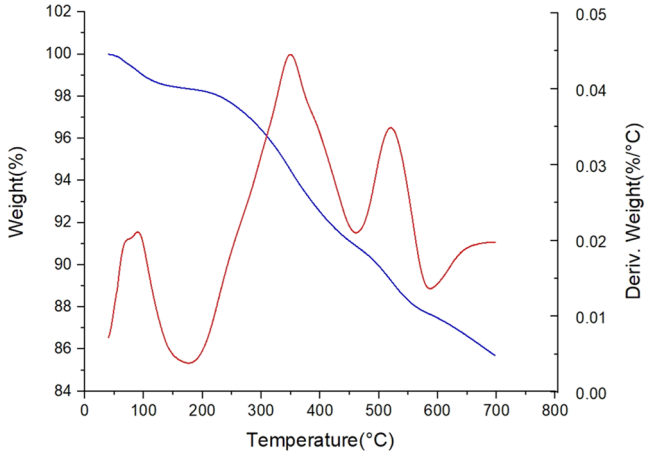

Figure 6. Thermogravimetric (TG) and derivative thermogravimetric (DTG) analyses of Fe_3O_4@MIL-53(Al)-N(CH_2PO_3)$_2$.

work Fe_3O_4@MIL-53(Al)-N(CH_2PO_3)$_2$ (Scheme 2). In this report, the solvothermal method was used to prepare Al-based MOFs to show the diversity of the method for the synthesis of the described MOFs. In addition to being porous and having phosphorous acid groups, this catalyst has magnetic properties and can be easily separated from the reaction medium after the reaction is completed using an external magnet. For confirming the structure and morphology of the catalyst, various techniques such as energy-dispersive X-ray spectroscopy (EDS), N_2 adsorption−desorption isotherms (BET), FT-IR spectroscopy, XRD, SEM elemental mapping, vibrating sample magnetometry (VSM), thermal gravimetry (TG), and

https://doi.org/10.1021/acsomega.2c06651
ACS Omega 2023, 8, 18479−18490

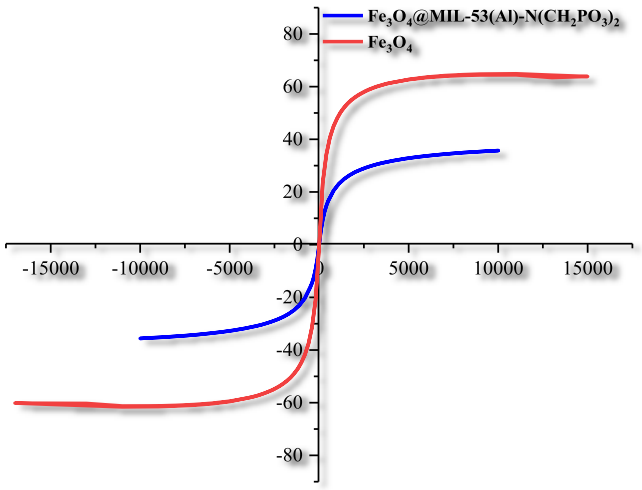

Figure 7. Vibrating sample magnetometry (VSM) of Fe_3O_4 and Fe_3O_4@MIL-53(Al)-N$(CH_2PO_3)_2$.

Table 1. Effect of Different Amounts of Catalyst, Temperature, and Solvent on the Synthesis of Fused Nicotinonitrile Derivatives

entry	solvent	time (min)	cat. (mg)	temp. (°C)	yield (%)
1		50	20	110	85
2		80	10	110	70
3		120	5	110	30
4		65	15	110	45
5		60	30	110	82
6		180		110	15
7		180	20	25	
8		120	20	50	25
9		100	20	80	42
10		65	20	100	72
11		50	20	120	80
12	*n*-hexane	180	20	reflux	
13	EtOH	120	20	reflux	72
14	MeOH	120	20	reflux	65
15	DMF	100	20	110	70
16	CH_2Cl_2	180	20	reflux	
17	$CHCl_3$	180	20	reflux	
18	CH_3CN	120	20	reflux	42
19	EtOAc	180	20	reflux	
20	H_2O	120	20	reflux	27

derivative thermal gravimetry (DTG) were used. Synthesis of pyridines with various substitutions to yield biologically active candidates is our main research interest. In addition, the synthesis of susceptible molecules for the development of the anomeric-based oxidation concept is our other research target. Here, we tried to combine both of the abovementioned research interests.

The FT-IR spectra of the intermediate material, substrate, and catalyst are compared in Figure 2. According to the FT-IR spectra, the functional groups of MIL-53(Al)-NH_2 match with previously reported results.[20,39] The peaks at 3503 and 3384 cm^{-1} in MIL-53(Al)-NH_2 indicate the NH_2 functional group. The broad peak at 2700−3600 cm^{-1} indicates the acidic OH of PO_3H_2 and the Fe_3O_4 functional group in the catalyst. The adsorption bands at 1020−1180 cm^{-1} are related to P−O bond stretching. Also, the absorption band at 598 cm^{-1} is linked to the stretching vibration of the Fe−O group in Fe_3O_4. The changes of MIL-53(Al)-NH_2, MIL-53(Al)-N$(CH_2PO_3H_2)_2$, and Fe_3O_4@MIL-53(Al)-N$(CH_2PO_3)_2$ were detected in the synthesis of catalyst.

The morphology of Fe_3O_4@MIL-53(Al)-N$(CH_2PO_3)_2$ was studied using XRD, EDX spectroscopy, and SEM techniques. For this purpose, a comparative XRD analysis of Fe_3O_4@MIL-53(Al)-N$(CH_2PO_3)_2$ and MIL-53(Al)-NH_2 was performed, as shown in Figure 3. According to the XRD spectra, the structure of MIL-53(Al)-NH_2 matches well with previously reported studies.[20,39] The peaks corresponding to the regions of 2θ = 8.84, 10.44, 15.58, 18.04, 20.64, 26.99, and 48.28° indicate MIL-53(Al)-NH_2, and these peaks are also present in the final catalyst. On adding Fe_3O_4, the peaks of this compound at 2θ = 18.19, 30.09, 35.54, 43.14, 53.64, 57.39, 62.99, and 74.44° corresponding to the Fe_3O_4 diffraction lines (111), (220), (311), (400), (422), (511), (440), and (533) were included,[40] indicating the proper addition of Fe_3O_4 to MIL-53(Al)-NH_2. The XRD pattern of the catalyst shows that it has a crystalline nature. The size of the crystal and average interplaner distance were calculated by the Scherer equation and the Bragg equation, which are determined to be in the range of 6.8−13.4 nm. The results are shown in Table S1.

In another investigation, the scaffold catalyst was composed of C, N, O, Al, Fe, and P according to the energy-dispersive X-ray spectroscopy (EDX) technique (Figure 4). Also, the distribution of elements including C (red), N (blue), O (green), Al (yellow), Fe (gray), and P (orange) on the surface of the catalyst was investigated and verified by SEM elemental mapping (Figure 4). Therefore, energy-dispersive X-ray (EDX) spectroscopy and SEM elemental mapping of all of the expected elements confirm the uniform distribution of the elements on the surface.

Also, the scanning electron microscopy (SEM) technique was used to determine the morphology and particle size of the Fe_3O_4@MIL-53(Al)-N$(CH_2PO_3)_2$ catalyst, as shown in Figure 5. A comparison of the SEM images of Fe_3O_4@MIL-53(Al)-N$(CH_2PO_3)_2$ and MIL-53(Al)-NH_2 shows that the morphology has not changed after functionalization. According to SEM images, the particles of Fe_3O_4@MIL-53(Al)-N$(CH_2PO_3)_2$ were uniform in size, with good dispersion performance and no agglomeration.

The nitrogen adsorption−desorption isotherm (BET) of Fe_3O_4@MIL-53(Al)-N$(CH_2PO_3)_2$ is shown in Figure S1. This isotherm shows that the addition of Fe_3O_4 to MIL-53(Al)-N$(CH_2PO_3H_2)_2$ reduces the pore size and surface area up to 58.40 m^2/g. Also, the total pore volume of Fe_3O_4@MIL-53(Al)-N$(CH_2PO_3)_2$ is reduced to 0.248 cm^3/g.[20] The pore size distribution of Fe_3O_4@MIL-53(Al)-N$(CH_2PO_3)_2$ based on the BJH method is shown in Figure S1. The mean pore diameter of Fe_3O_4@MIL-53(Al)-N$(CH_2PO_3)_2$ is 17.02 nm.

To study the thermal stability of nanomagnetic metal−organic frameworks, thermogravimetric (TG) and derivative thermogravimetric (DTG) analyses were performed (Figure 6). Three stages of weight loss for Fe_3O_4@MIL-53(Al)-N$(CH_2PO_3)_2$ are observed. The first weight loss is related to the evaporation of organic solvents at 100 °C. The main weight loss at 350 °C can be assigned to the decomposition of the material including MIL-53(Al)-N$(CH_2PO_3H_2)_2$.

In continuity, magnetic measurement of Fe_3O_4@MIL-53(Al)-N$(CH_2PO_3)_2$ and Fe_3O_4 was performed using vibrating sample magnetometry (VSM) technique (Figure 7). According to the curves shown in Figure 7, magnetic measurements were performed for Fe_3O_4@MIL-53(Al)-N$(CH_2PO_3)_2$ 33.20 μg^{-1}

https://doi.org/10.1021/acsomega.2c06651
ACS Omega 2023, 8, 18479−18490

Table 2. Synthesis of Nicotinonitrile Derivatives (1b−14b) Using Fe_3O_4@MIL-53(Al)-N$(CH_2PO_3)_2$[41,42]

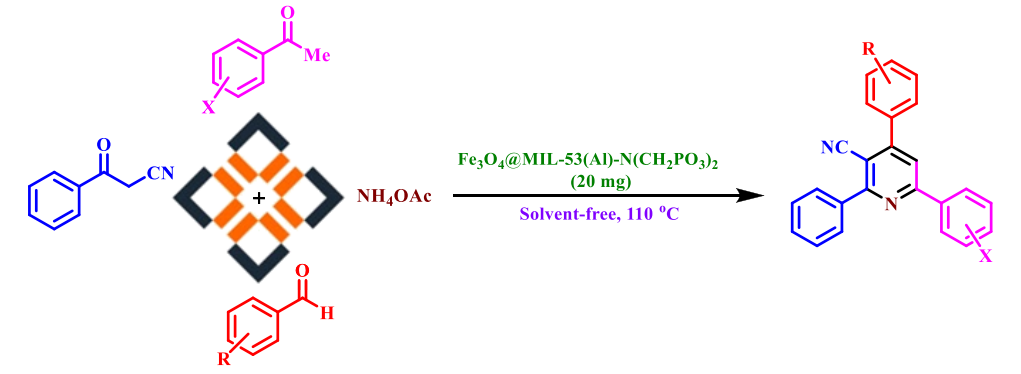

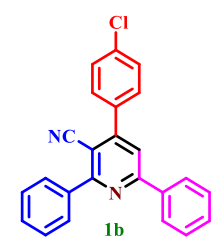

M.P (°C): 232-234[41]
Yield (%): 85
Time (min): 50

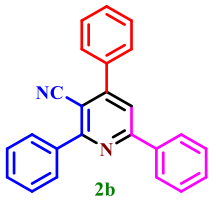

M.P (°C): 218-220[42]
Yield (%): 90
Time (min): 40

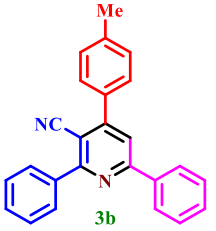

M.P (°C): 160-162[41]
Yield (%): 79
Time (min): 45

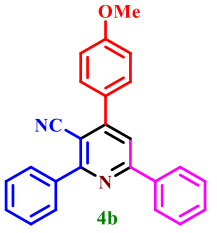

M.P (°C): 180-182[42]
Yield (%): 83
Time (min): 60

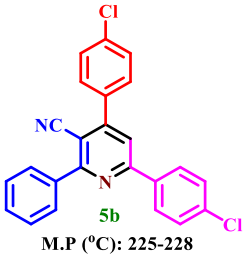

M.P (°C): 225-228
Yield (%): 87
Time (min): 45

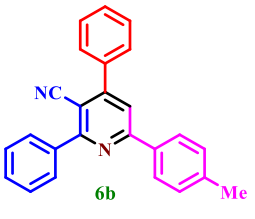

M.P (°C): 215-218[41]
Yield (%): 82
Time (min): 55

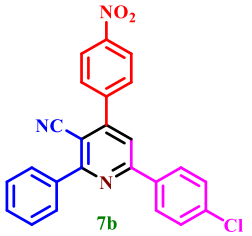

M.P (°C): 265-268
Yield (%): 74
Time (min): 50

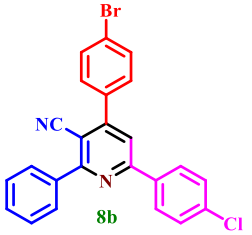

M.P (°C): 218-220
Yield (%): 80
Time (min): 50

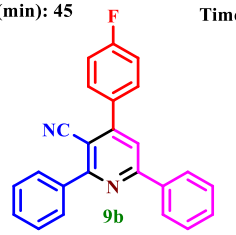

M.P (°C): 230-232[41]
Yield (%): 80
Time (min): 45

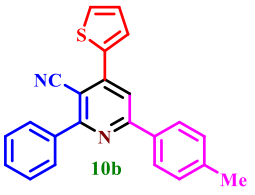

M.P (°C): 160-162
Yield (%): 72
Time (min): 40

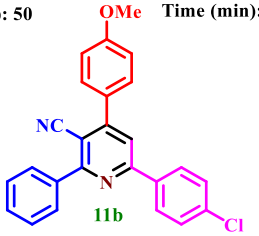

M.P (°C): 197-200
Yield (%): 74
Time (min): 55

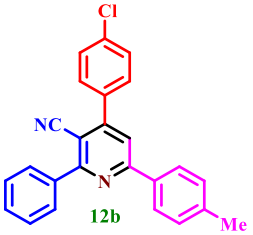

M.P (°C): 225-228[41]
Yield (%): 76
Time (min): 50

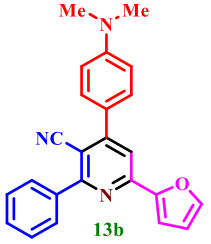

M.P (°C): 240-242
Yield (%): 68
Time (min): 60

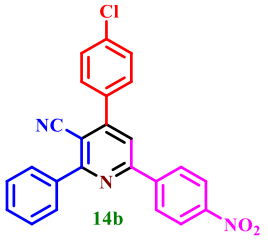

M.P (°C): >300
Yield (%): 82
Time (min): 50

and Fe_3O_4 66.5 μg^{-1}. This decrease is due to the coating of Fe_3O_4 nanoparticles by MIL-53(Al)-N$(CH_2PO_3H_2)_2$.

After the successful synthesis and characterization of Fe_3O_4@MIL-53(Al)-N$(CH_2PO_3)_2$, it was used for the preparation of nicotinonitrile derivatives. The abovementioned

https://doi.org/10.1021/acsomega.2c06651
ACS Omega 2023, 8, 18479−18490

Table 3. Synthesis of Nicotinonitrile Derivatives (1c−13c) Using Fe_3O_4@MIL-53(Al)-N(CH_2PO_3)$_2$

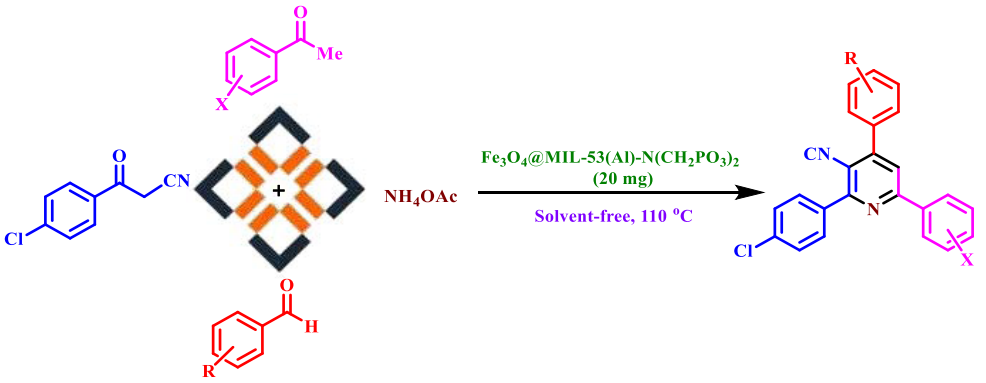

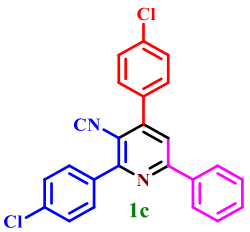

M.P (°C): 270-272
Yield (%): 88
Time (min): 45

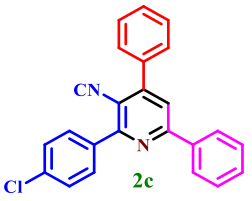

M.P (°C): 245-248[41]
Yield (%): 86
Time (min): 40

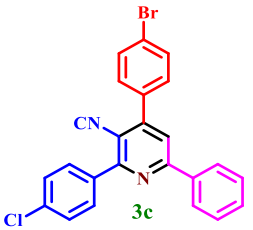

M.P (°C): 200-202[41]
Yield (%): 76
Time (min): 45

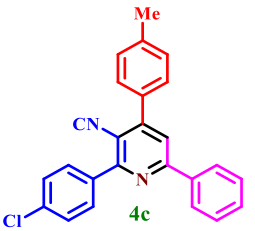

M.P (°C): 255-257
Yield (%): 83
Time (min): 40

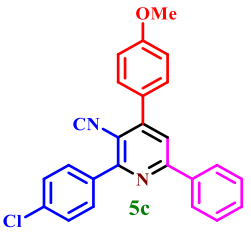

M.P (°C): 235-237
Yield (%): 84
Time (min): 60

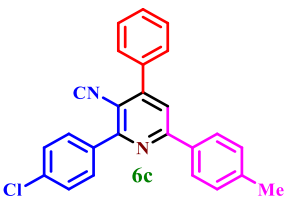

M.P (°C): 215-217
Yield (%): 85
Time (min): 55

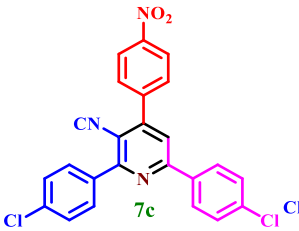

M.P (°C): 275-278
Yield (%): 74
Time (min): 60

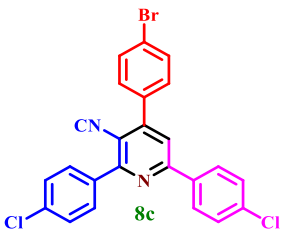

M.P (°C): 230-232
Yield (%): 77
Time (min): 45

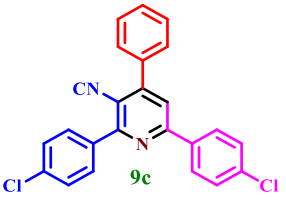

M.P (°C): 195-198
Yield (%): 82
Time (min): 45

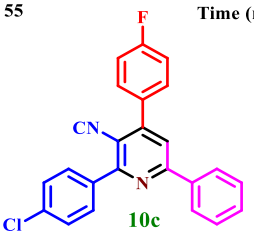

M.P (°C): 232-234
Yield (%): 84
Time (min): 60

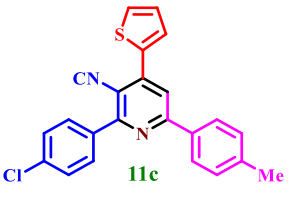

M.P (°C): 235-238
Yield (%): 74
Time (min): 60

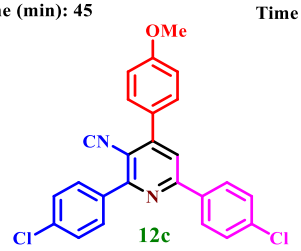

M.P (°C): 230-232
Yield (%): 80
Time (min): 40

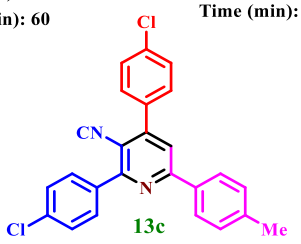

M.P (°C): 180-182[41]
Yield (%): 79
Time (min): 50

catalyst was applied for the multicomponent reaction of 3-oxo-3-phenylpropanenitrile (1 mmol, 0.145 g), acetophenone (1 mmol, 0.120 g), 4-chlorobenzaldehyde (1 mmol, 0.140 g), and ammonium acetate (1.5 mmol, 0.115 g) as a model reaction via a cooperative vinylogous anomeric-based oxidation. The model reaction was tested using different amounts of catalysts,

https://doi.org/10.1021/acsomega.2c06651
ACS Omega 2023, 8, 18479−18490

Scheme 4. Proposed Mechanism for the Synthesis of Nicotinonitriles Using Fe_3O_4@MIL-53(Al)-N(CH_2PO_3)$_2$

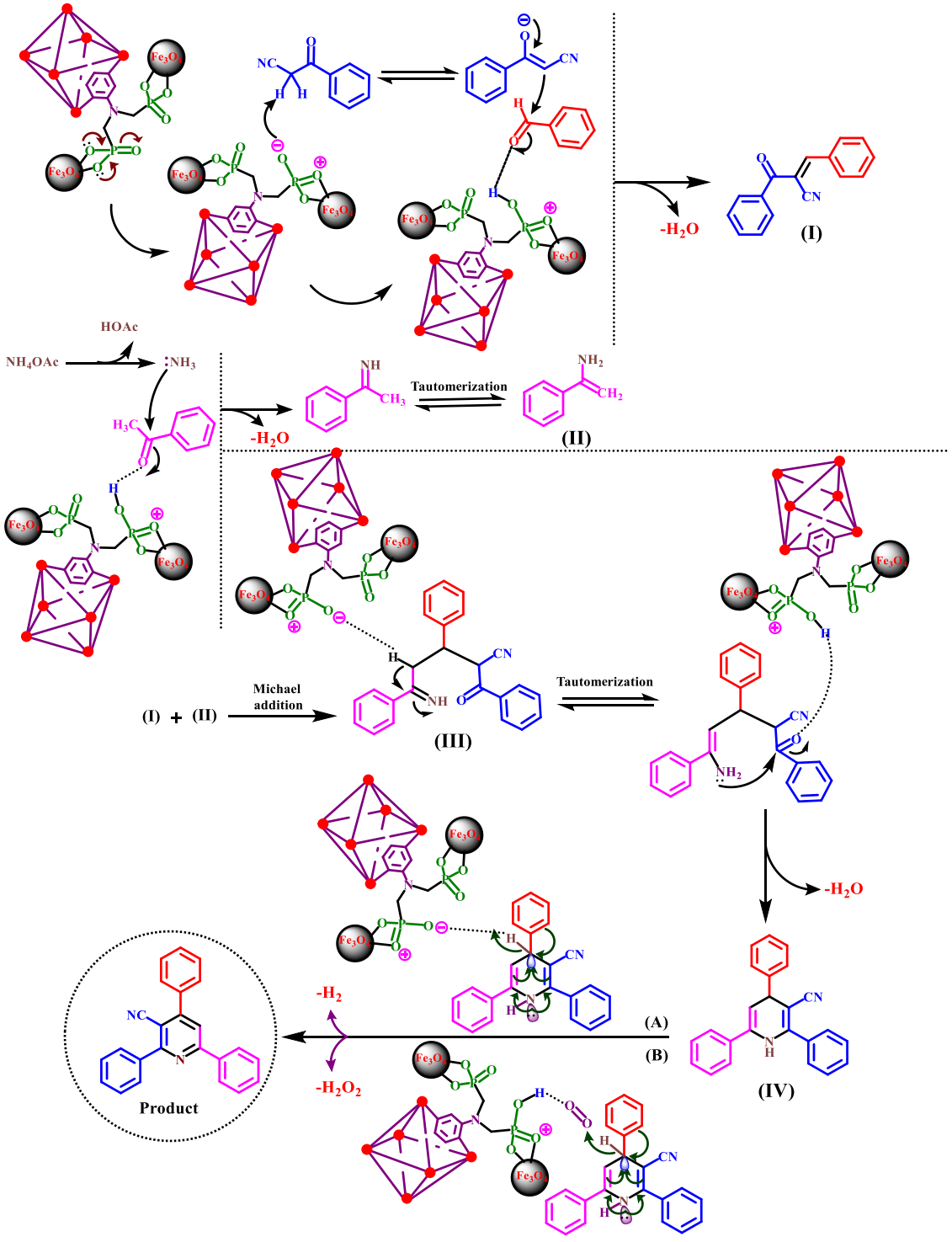

solvents, and temperatures. The results of the obtained products are summarized in Table 1. The best parameters for the synthesis of nicotinonitrile were achieved in the presence of Fe_3O_4@MIL-53(Al)-N(CH_2PO_3)$_2$ (20 mg) at 110 °C under solvent-free conditions (entry 1, Table 1). The model reaction was also tested using different organic solvents such as *n*-hexane, MeOH, EtOH, CH_3CN, CH_2Cl_2, EtOAc, DMF, $CHCl_3$, and water (5 mL), the results obtained for which did not improve entries 12−20 in Table 1. Results show that Fe_3O_4@MIL-53(Al)-N(CH_2PO_3)$_2$ is suitable for the preparation of nicotinonitrile derivatives. Besides, the model reaction was tested for the preparation of the target reaction under N_2 and Ar atmospheres for confirming anomeric-based oxidation (ABO). The reaction was successfully performed in the absence of any oxygen molecules.

After the optimization of the reaction conditions, the efficiency and applicability of Fe_3O_4@MIL-53(Al)-N-(CH_2PO_3)$_2$ were studied for the preparation of nicotinonitriles. The results summarized in Tables 2 and 3 indicate that starting materials (3-oxo-3-phenylpropanenitrile or 3-(4-

https://doi.org/10.1021/acsomega.2c06651
ACS Omega 2023, 8, 18479−18490

Table 4. Evaluation of Various Catalysts for the Synthesis of Nicotinonitriles in Comparison with Fe_3O_4@MIL-53(Al)-$N(CH_2PO_3)_2$

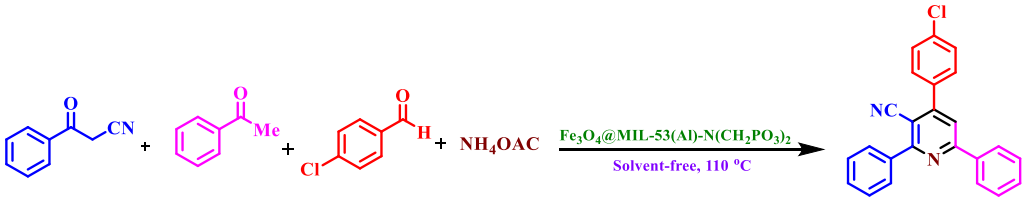

entry	catalyst	amount of catalyst	time (min)	yield (%)
1	SSA[44]	20 mg	100	30
2	NaOH	20 mol %	150	32
3	Fe_3O_4	20 mg	120	trace
4	*p*-TSA	20 mol %	120	35
5	pipyridine	20 mol %	100	trace
6	nano-SB-[PSIM]Cl[45]	20 mg	180	
7	GTBSA[46]	20 mol %	120	55
8	APVPB[47]	20 mg	100	40
9	[Py-SO_3H]Cl[48]	20 mol %	80	48
10	[PVI-SO_3H]Cl[49]	20 mg	180	28
11	Et_3N	20 mol %	120	32
12	GTMPA[22]	20 mol %	120	55
13	$NaHSO_4$	20 mol %	60	77
14	Fe_3O_4	20 mg	120	trace
15	MIL-53(Al)-NH_2	20 mg	120	25
16	MIL-53(Al)-$N(CH_2PO_3H_2)_2$	20 mg	60	80
17	Fe_3O_4@MIL-53(Al)-$N(CH_2PO_3)_2$, this work	20 mg	50	85

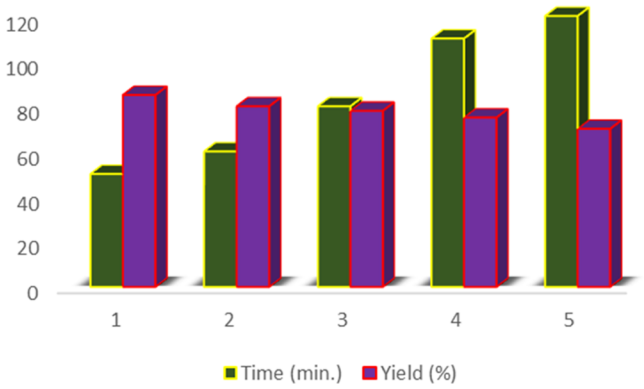

Figure 8. Recyclability of Fe_3O_4@MIL-53(Al)-$N(CH_2PO_3)_2$ for the synthesis of nicotinonitrile derivatives.

chlorophenyl)-3-oxopropanenitrile) and various aldehydes including those bearing electron-donating, electron-withdrawing, and halogen groups afforded desired products (**1b−14b**) and (**1c−13c**) in excellent yields (68−90%) and short reaction times (40−60 min).

In the suggested mechanism, the starting material [(3-oxo-3-phenylpropanenitrile or 3-(4-chlorophenyl)-3-exopropanenitrile)] is activated by the catalyst. The enol form of the starting material and activated aldehyde produced intermediate I. On the other hand, the ammonia generated from ammonium acetate reacts with activated acetophenone to form intermediate II. Then, the reaction between intermediates I and II leads to intermediate III. Subsequently, intermediate III creates intermediate IV by an intramolecular reaction and loss of one molecule of H_2O. In the last stage of the reaction mechanism, intermediate IV is converted into the final product through two possible paths A and/or B, via a cooperative vinylogous anomeric-based oxidation mechanism, releasing H_2 or H_2O_2 (Scheme 4).[34,35,43] Also, to investigate the activation of aldehyde by the catalyst, *p*-chlorobenzaldehyde was reacted with Fe_3O_4@MIL-53(Al)-$N(CH_2PO_3)_2$ at room temperature. Then, the FT-IR spectra of the reaction mixtures were examined. The absorption band of C═O of *p*-chlorobenzaldehyde at 1693 cm^{-1} shifted to 1693, 1695, 1701, and 1705 cm^{-1} in the presence of MIL-53(Al)-NH_2, Fe_3O_4, MIL-53(Al)-$N(CH_2PO_3H_2)_2$, and Fe_3O_4@MIL-53(Al)-$N(CH_2PO_3)_2$, respectively (Figure S2).

Following the optimal synthesis of nicotinonitrile derivatives by Fe_3O_4@MIL-53(Al)-$N(CH_2PO_3)_2$, we tested 3-oxo-3-phenylpropanenitrile (1 mmol, 0.145 g), acetophenone (1 mmol, 0.120 g), 4-chlorobenzaldehyde (1 mmol, 0.140 g), and ammonium acetate (1.5 mmol, 0.12 g) as model reactions using various inorganic and organic catalysts (solid acids, nanomagnetic liquids, and ionic liquids). According to the results shown in Table 4, it can be concluded that Fe_3O_4@MIL-53(Al)-$N(CH_2PO_3)_2$ exhibits the best performance compared to other catalysts. To prove the recyclability of the catalyst, we tested the model reaction under optimal conditions. The results in Figure 8 show that the Fe_3O_4@MIL-53(Al)-$N(CH_2PO_3)_2$ catalyst can be reused up to five times without a noticeable change in its catalytic activity. To prove the stability of the catalyst, FT-IR and XRD analyses were performed, and the corresponding spectra of fresh and reused catalysts are compared in Figures S3 and S4. The pattern of the reused catalyst is the same as the profile of the fresh catalyst without apparent loss of crystallinity. Also, Fe and Al loadings at the synthesized MOF were determined by ICP analysis. For this purpose, ICP results confirmed that the synthesized magnetic porous catalyst contains 6862.80×10^{-6} mol/g Al and 3183.46×10^{-6} mol/g Fe.

https://doi.org/10.1021/acsomega.2c06651
ACS Omega 2023, 8, 18479−18490

CONCLUSIONS

In conclusion, a new nanomagnetic metal−organic framework Fe_3O_4@MIL-53(Al)-N$(CH_2PO_3)_2$ was prepared and introduced via a post-modification method. The synthesized nanomagnetic metal−organic framework was fully characterized by FT-IR, SEM elemental mapping, EDX, XRD, SEM, TGA−DTG, N_2 adsorption−desorption, BJH, and VSM. It was used in the preparation of nicotinonitrile derivatives as biologically active candidates with a high yield and short reaction time. The recyclability and reusability of the presented catalyst, green conditions, and easy work-up are major advantages of the described methodology.

ASSOCIATED CONTENT

Supporting Information

The Supporting Information is available free of charge at https://pubs.acs.org/doi/10.1021/acsomega.2c06651.

Spectral data of nicotinonitriles, different kinds of anomeric effects, XRD data and N_2 adsorption−desorption isotherms of the catalyst, FT-IR spectra of *p*-Cl-benzaldehyde in the presence of different stages of the catalyst, and comparison of FT-IR and XRD spectra of the fresh and reused catalyst (PDF)

AUTHOR INFORMATION

Corresponding Authors

Mahmoud Zarei − *Department of Chemistry, Faculty of Science, University of Qom, Qom 37185-359, Iran;* orcid.org/0000-0002-3701-9755; Email: mahmoud8103@yahoo.com

Mohammad Ali Zolfigol − *Department of Organic Chemistry, Faculty of Chemistry, Bu-Ali Sina University, Hamedan 65178-38683, Iran;* orcid.org/0000-0002-4970-8646; Phone: +988138282807; Email: zolfi@basu.ac.ir, mzolfigol@yahoo.com; Fax: +988138380709

Authors

Bashirullah Danishyar − *Department of Organic Chemistry, Faculty of Chemistry, Bu-Ali Sina University, Hamedan 65178-38683, Iran*

Hassan Sepehrmansourie − *Department of Organic Chemistry, Faculty of Chemistry, Bu-Ali Sina University, Hamedan 65178-38683, Iran*

Hossein Ahmadi − *Department of Organic Chemistry, Faculty of Chemistry, Bu-Ali Sina University, Hamedan 65178-38683, Iran*

Mojtaba Hosseinifard − *Department of Energy, Materials and Energy Research Center, Karaj 31648-19712, Iran;* orcid.org/0000-0003-3770-5963

Complete contact information is available at: https://pubs.acs.org/10.1021/acsomega.2c06651

Notes

The authors declare no competing financial interest.

ACKNOWLEDGMENTS

The authors thank the Bu-Ali Sina University and Iran National Science Foundation (INSF) (Grant Number 4004528) for financial support.

REFERENCES

(1) Stock, N.; Biswas, S. Synthesis of metal-organic frameworks (MOFs): routes to various MOF topologies, morphologies, and composites. *Chem. Rev.* **2012**, *112*, 933−969.

(2) Kitagawa, S.; Kitagawa, S. Metal-organic frameworks (MOFs). *Chem. Soc. Rev.* **2014**, *43*, 5415−5418.

(3) (a) Wang, S.; McGuirk, C. M.; d'Aquino, A.; Mason, J. A.; Mirkin, C. A. Metal-organic framework nanoparticles. *Adv. Mater.* **2018**, *30*, No. 1800202. (b) Kaushal, S.; Kaur, G.; Kaur, J.; Singh, P. P. First transition series metal-organic frameworks: synthesis, properties and applications. *Mater. Adv.* **2021**, *2*, 7308−7335.

(4) Perry, J. J., IV; Perman, J. A.; Zaworotko, M. J. Design and synthesis of meta-organic frameworks using metal-organic polyhedra as supermolecular building blocks. *Chem. Soc. Rev.* **2009**, *38*, 1400−1417.

(5) Li, H.; Eddaoudi, M.; O'Keeffe, M.; Yaghi, O. M. Design and synthesis of an exceptionally stable and highly porous metal-organic framework. *Nature* **1999**, *402*, 276−279.

(6) (a) Singh, S.; Kaushal, S.; Kaur, J.; Kaur, G.; Mittal, S. K.; Singh, P. P. CaFu MOF as an efficient adsorbent for simultaneous removal of imidacloprid pesticide and cadmium ions from wastewater. *Chemosphere* **2021**, *272*, No. 129648. (b) Lázaro, I. A.; Forgan, R. S. Application of zirconium MOFs in drug delivery and biomedicine. *Coord. Chem. Rev.* **2019**, *380*, 230−259.

(7) (a) Ozen, H. A.; Ozturk, B. Gas separation characteristic of mixed matrix membrane prepared by MOF-5 including different metals. *Sep. Purif. Technol.* **2019**, *211*, 514−521. (b) Hu, J.; Chen, Y.; Zhang, H.; Chen, Z.; Ling, Y.; Yang, Y.; Liu, X.; Jia, Y.; Zhou, Y. TEA-assistant synthesis of MOF-74 nanorods for drug delivery and in-vitro magnetic resonance imaging. *Microporous Mesoporous Mater.* **2021**, *315*, No. 110900.

(8) (a) Zhu, L.; Liu, X. Q.; Jiang, H. L.; Sun, L. B. Metal-organic frameworks for heterogeneous basic catalysis. *Chem. Rev.* **2017**, *117*, 8129−8176. (b) Sharma, A.; Verma, K.; Kaushal, S.; Badru, R. A novel 2-D accordion like Al-BPED MOF as reusable and selective catalyst for *N*-alkylation of amines with dialkylcarbonates. *Appl. Organomet. Chem.* **2022**, *36*, No. e6814.

(9) (a) Sepehrmansourie, H. Metal-organic frameworks (MOFs): as multi-purpose catalysts. *Iran. J. Catal.* **2021**, *11*, 207. (b) Sepehrmansourie, H.; Alamgholiloo, H.; Pesyan Noroozi Pesyan, N.; Zolfigol, M. A. A MOF-on-MOF strategy to construct double Z-scheme heterojunction for high-performance photocatalytic degradation. *Appl. Catal. B: Environ.* **2022**, *321*, No. 122082. (c) Sepehrmansourie, H.; Zarei, M.; Zolfigol, M. A.; Kalhor, S.; Shi, H. Catalytic chemo and homoselective ipso-nitration under mild condition. *Mol. Catal.* **2022**, *531*, No. 112634.

(10) Sepehrmansourie, H.; Zarei, M.; Zolfigol, M. A.; Babaee, S.; Rostamnia, S. Application of novel nanomagnetic metal-organic frameworks as a catalyst for the synthesis of new pyridines and 1, 4-dihydropyridines via a cooperative vinylogous anomeric based oxidation. *Sci. Rep.* **2021**, *11*, No. 5279.

(11) Zhang, S.; Zhao, X.; Niu, H.; Shi, Y.; Cai, Y.; Jiang, G. Superparamagnetic Fe_3O_4 nanoparticles as catalysts for the catalytic oxidation of phenolic and aniline compounds. *J. Hazard. Mater.* **2009**, *167*, 560−566.

(12) (a) Kurmoo, M. Magnetic metal-organic frameworks. *Chem. Soc. Rev.* **2009**, *38*, 1353−1379. (b) Taghavi, R.; Rostamnia, S.; Farakzadeh, M.; et al. Magnetite Metal−Organic Frameworks: Applications in Environmental Remediation of Heavy Metals, Organic Contaminants, And Other Pollutants. *Inorg. Chem.* **2022**, *61*, 15747−15783. (c) Farzaneh, F.; Sadeghi, Y. Immobilized V-MIL-101 on modified Fe_3O_4 nanoparticles as heterogeneous catalyst for epoxidation of allyl alcohols and alkenes. *J. Mol. Catal. A* **2015**, *398*, 275−281.

(13) Vojvodic, A.; Nørskov, J. K. New design paradigm for heterogeneous catalysts. *Natl. Sci. Rev.* **2015**, *2*, 140−143.

(14) Mondloch, J. E.; Bayram, E.; Finke, R. G. A review of the kinetics and mechanisms of formation of supported-nanoparticle heterogeneous catalysts. *J. Mol. Catal. A* **2012**, *355*, 1−38.

(15) Shi, Z.; Xu, C.; Guan, H.; Li, L.; Fan, L.; Wang, Y.; Liu, L.; Meng, Q.; Zhang, R. Magnetic metal organic frameworks (MOFs) composite for removal of lead and malachite green in wastewater. *Colloids Surf., A* **2018**, *539*, 382−390.
(16) (a) Sepehrmansourie, H.; Zarei, M.; Zolfigol, M. A.; Babaee, S.; Azizian, S.; Rostamnia, S. Catalytic synthesis of new pyrazolo [3, 4-*b*] pyridine via a cooperative vinylogous anomeric-based oxidation. *Sci. Rep.* **2022**, *12*, 5279. (b) Ma, J.; Li, S.; Wu, G.; Arabi, M.; Tan, F.; Guan, Y.; Li, J.; Chen, L. Preparation of magnetic metal-organic frameworks with high binding capacity for removal of two fungicides from aqueous environments. *J. Ind. Eng. Chem.* **2020**, *90*, 178−189.
(17) Jalili, F.; Zarei, M.; Zolfigol, M. A.; Khazaei, A. Application of novel metal-organic framework [Zr-UiO-66-PDC-SO_3H]$FeCl_4$ in the synthesis of dihydrobenzo [*g*] pyrimido [4, 5-*b*] quinoline derivatives. *RSC Adv.* **2022**, *12*, 9058−9068.
(18) Kalhor, S.; Zarei, M.; Sepehrmansourie, H.; Zolfigol, M. A.; Shi, H.; Wang, J.; Arjomandi, J.; Hasani, M.; Schirhagl, R. Novel uric acid-based nano organocatalyst with phosphorous acid tags: application for synthesis of new biologically-interest pyridines with indole moieties via a cooperative vinylogous anomeric based oxidation. *Mol. Catal.* **2021**, *507*, No. 111549.
(19) (a) Sepehrmansouri, H.; Zarei, M.; Zolfigol, M. A.; Moosavi-Zare, A. R.; Rostamnia, S.; Moradi, S. Multilinker phosphorous acid anchored En/MIL-100(Cr) as a novel nanoporous catalyst for the synthesis of new *N*-heterocyclic pyrimido [4, 5-*b*] quinolines. *Mol. Catal.* **2020**, *481*, No. 110303. (b) Tavakoli, E.; Sepehrmansourie, H.; Zarei, M.; Zolfigol, M. A.; Khazaei, A.; Hosseinifard, M. Applications of novel composite UiO-66-NH_2/Melamine with phosphorous acid tags as a porous and efficient catalyst for the preparation of novel spiro-oxindoles. *New J. Chem.* **2022**, *46*, 19054−19061. (c) Sepehrmansourie, H.; Kalhor, S.; Zarei, M.; Zolfigol, M. A.; Hosseinifard, M. A convenient catalytic method for preparation of new tetrahydropyrido[2,3-*d*]pyrimidines via a cooperative vinylogous anomeric based oxidation. *RSC Adv.* **2022**, *12*, 34282−34292.
(20) (a) Kalhor, S.; Zarei, M.; Zolfigol, M. A.; Sepehrmansourie, H.; Nematollahi, D.; Alizadeh, S.; Shi, H.; Arjomandi, J. Anodic electrosynthesis of MIL-53(Al)-N(CH_2PO3H_2)2 as a mesoporous catalyst for synthesis of novel (*N*-methyl-pyrrol)-pyrazolo [3, 4-*b*] pyridines via a cooperative vinylogous anomeric based oxidation. *Sci. Rep.* **2021**, *11*, No. 19370. (b) An, Y.; Li, H.; Liu, Y.; Huang, B.; Sun, Q.; Dai, Y.; Qin, X.; Zhang, X. Photoelectrical, photophysical and photocatalytic properties of Al based MOFs: MIL-53 (Al) and MIL-53-NH_2 (Al). *J. Solid State Chem.* **2016**, *233*, 194−198.
(21) Afsar, J.; Zolfigol, M. A.; Khazaei, A.; Zarei, M.; Gu, Y.; Alonso, D. A.; Khoshnood, A. Synthesis and application of melamine-based nano catalyst with phosphonic acid tags in the synthesis of (3′-indolyl) pyrazolo [3, 4-*b*] pyridines via vinylogous anomeric based oxidation. *Mol. Catal.* **2020**, *482*, No. 110666.
(22) Moradi, S.; Zolfigol, M. A.; Zarei, M.; Alonso, D. A.; Khoshnood, A. Synthesis of a biological-based glycoluril with phosphorous acid tags as a new nanostructured catalyst: application for the synthesis of novel natural henna-based compounds. *ChemistrySelect* **2018**, *3*, 3042−3047.
(23) Rasooll, M. M.; Zarei, M.; Zolfigol, M. A.; Sepehrmansourie, H.; Omidi, A.; Hasani, M.; Gu, Y. Novel nano-architectured carbon quantum dots (CQDs) with phosphorous acid tags as an efficient catalyst for the synthesis of multisubstituted 4*H*-pyran with indole moieties under mild conditions. *RSC Adv.* **2021**, *11*, 25995−26007.
(24) Jalili, F.; Zarei, M.; Zolfigol, M. A.; Rostamnia, S.; Moosavi-Zare, A. R. SBA-15/PrN $(CH_2PO_3H_2)_2$ as a novel and efficient mesoporous solid acid catalyst with phosphorous acid tags and its application on the synthesis of new pyrimido [4, 5-*b*] quinolones and pyrido [2, 3-*d*] pyrimidines via anomeric based oxidation. *Microporous Mesoporous Mater.* **2020**, *294*, No. 109865.
(25) Moosavi-Zare, A. R.; Zolfigol, S.; Zare, A.; Pourali, A. R.; Ayazi-Nasrabadi, R.; et al. Synthesis of 2, 4, 6-triarylpyridines using $ZrOCl_2$ under solvent-free conditions. *Synlett* **2014**, *25*, 193−196.
(26) Liu, Y.; Yang, D.; Hong, Z.; Guo, S.; Liu, M.; Zuo, D.; Ge, D.; Qin, M.; Sun, D. Synthesis and biological evaluation of 4, 6-diphenyl-2-(1*H*-pyrrol-1-yl) nicotinonitrile analogues of crolibulin and combretastatin A-4. *Eur. J. Med. Chem.* **2018**, *146*, 185−193.
(27) Shamroukh, A. H.; Kotb, E. R.; Anwar, M. M.; Sharaf, M. Review on the chemistry of nicotinonitriles and their applications. *Egypt. J. Chem.* **2021**, *64*, 4509−4529.
(28) Rakshin, S. O.; Odin, I. S.; Sosnin, I. M.; Zatynatskiy, E. A.; Ostapenko, G. I.; Golovanov, A. A. Synthesis and fluorescence properties of nicotinonitrile 1, 2, 3-triazole derivatives. *Russ. Chem. Bull.* **2018**, *67*, 1710−1715.
(29) Gouda, M. A.; Hussein, B. H.; Helal, M. H.; Salem, M. A. A Review: synthesis and medicinal importance of nicotinonitriles and their analogous. *J. Heterocycl. Chem.* **2018**, *55*, 1524−1553.
(30) Juaristi, E.; Cuevas, G. Recent studies of the anomeric effect. *Tetrahedron* **1992**, *48*, 5019−5087.
(31) Katritzky, A. R.; Steel, P. J.; Denisenko, S. N. X-Ray crystallographic evidence for a vinylogous anomeric effect in benzotriazole-substituted heterocycles. *Tetrahedron* **2001**, *57*, 3309−3314.
(32) Alabugin, I. V. *Stereoelectronic Effects: A Bridge Between Structure and Reactivity*, 1st ed.; John Wiley & Sons, 2016.
(33) Alabugin, I. V.; Kuhn, L.; Medvedev, M. G.; Krivoshchapov, N. V.; Vil, V. A.; Yaremenko, I. A.; Mehaffy, P.; Yarie, M.; Terent'ev, A. O.; Zolfigol, M. A. Stereoelectronic power of oxygen in control of chemical reactivity: the anomeric effect is not alone. *Chem. Soc. Rev.* **2021**, *50*, 10253.
(34) Alabugin, I. V.; Kuhn, L.; Krivoshchapov, N. V.; Mehaffy, P.; Medvedev, M. G. Anomeric effect, hyperconjugation and electrostatics: Lessons from complexity in a classic stereoelectronic phenomenon. *Chem. Soc. Rev.* **2021**, *50*, 10212.
(35) Yarie, M. Spotlight: Catalytic vinylogous anomeric based oxidation. *Iran. J. Catal.* **2020**, *10*, 79−83.
(36) Yarie, M. Catalytic anomeric based oxidation. *Iran. J. Catal.* **2017**, *7*, 85−88.
(37) (a) Hamasaka, G.; Tsuji, H.; Uozumi, Y. Organoborane-catalyzed hydrogenation of unactivated aldehydes with a Hantzsch ester as a synthetic NAD(P)H analogue. *Synlett* **2015**, *26*, 2037−2041. (b) He, T.; Shi, R.; Gong, Y.; Jiang, G.; Liu, M.; Qian, S.; Wang, Z. Base-promoted cascade approach for the preparation of reduced Knoevenagel adducts using hantzsch esters as reducing agent in water. *Synlett* **2016**, *27*, 1864−1869. (c) Bai, C.-B.; Wang, N. X.; Xing, Y.; Lan, X. W. Progress on chiral NAD(P)H model compounds. *Synlett* **2017**, *13*, 402−414.
(38) (a) Pandey, G.; Vaitla, J. Desulfonylative methenylation of *β*-keto sulfones. *Org. Lett.* **2015**, *17*, 4890−4893. (b) Sun, L.; Bera, H.; Chui, W. K. Synthesis of pyrazolo [1, 5-*a*][1, 3, 5] triazine derivatives as inhibitors of thymidine phosphorylase. *Eur. J. Med. Chem.* **2013**, *65*, 1−11.
(39) Moreno, J. M.; Velty, A.; Díaz, U.; Corma, A. Synthesis of 2D and 3D MOFs with tuneable Lewis acidity from preformed 1D hybrid sub-domains. *Chem. Sci.* **2019**, *10*, 2053−2066.
(40) Karimi, F.; Yarie, M.; Zolfigol, M. A. Fe_3O_4@SiO_2@$(CH_2)_3$-urea-thiourea: a novel hydrogen-bonding and reusable catalyst for the construction of bipyridine-5-carbonitriles via a cooperative vinylogous anomeric based oxidation. *Mol. Catal.* **2020**, *497*, No. 111201.
(41) Rakshit, A.; Kumar, P.; Alam, T.; Dhara, H.; Patel, B. K. Visible-light-accelerated Pd-catalyzed cascade addition/cyclization of arylboronic acids to *γ*- and *β*-Ketodinitriles for the construction of 3-cyanopyridines and 3-cyanopyrrole analogues. *J. Org. Chem.* **2020**, *85*, 12482−12504.
(42) Abdel-Aziz, A.-M. Lewis acid-promoted direct substitution of 2-methoxy-3-cyanopyridines by organo cuprates. Part 3: Facile preparation of nicotinamide and nicotinic acid derivatives. *Tetrahedron Lett.* **2007**, *48*, 2861−2865.
(43) Babaee, S.; Zarei, M.; Sepehrmansourie, H.; Zolfigol, M. A.; Rostamnia, S. Synthesis of metal-organic frameworks MIL-101(Cr)-NH_2 containing phosphorous acid functional groups: application for the synthesis of *N*-amino-2-pyridone and pyrano [2,3-*c*]pyrazole derivatives via a cooperative vinylogous anomeric-based oxidation. *ACS Omega* **2020**, *5*, 6240−6249.

https://doi.org/10.1021/acsomega.2c06651
ACS Omega 2023, 8, 18479−18490

(44) (a) Zolfigol, M. A. Silica sulfuric acid/$NaNO_2$ as a novel heterogeneous system for production of thionitrites and disulfides under mild conditions. *Tetrahedron* **2001**, *57*, 9509−9511. (b) Sepehrmansourie, H. Spotlight: silica sulfuric acid (SSA): as a multipurpose catalyst. *Iran. J. Catal.* **2020**, *10*, 175−179.
(45) Zare, A.; Merajoddin, M.; Moosavi-Zare, A. R.; Zarei, M.; Beyzavi, M. H.; Zolfigol, M. A. Design and characterization of nano-silica-bonded 3-n-propyl-1-sulfonic acid imidazolium chloride {nano-SB-[PSIM]Cl} as a novel, heterogeneous and reusable catalyst for the condensation of arylaldehydes with β-naphthol and alkyl carbamates. *Res. Chem. Intermed.* **2016**, *42*, 2365−2378.
(46) Zarei, M.; Sepehrmansourie, H.; Zolfigol, M. A.; Karamian, R.; Moazzami Farida, S. H. Novel nano-size and crab-like biological-based glycoluril with sulfonic acid tags as a reusable catalyst: its application to the synthesis of new mono- and bis-spiropyrans and their in vitro biological studies. *New. J. Chem.* **2018**, *42*, 14308−14317.
(47) Noroozizadeh, E.; Moosavi-Zare, A. R.; Zolfigol, M. A.; Zarei, M.; Karamian, R.; Asadbegy, M.; Yari, S.; Moazzami Farida, S. H. Synthesis of bis-coumarins over acetic acid functionalized poly(4-vinylpyridinum) bromide (APVPB) as a green and efficient catalyst under solvent-free conditions and their biological activity. *J. Iran. Chem. Soc.* **2018**, *15*, 471−481.
(48) Moosavi-Zare, A. R.; Zolfigol, M. A.; Zarei, M.; Zare, A.; Khakyzadeh, V.; Hasaninejad, A. Design, characterization and application of new ionic liquid 1-sulfopyridinium chloride as an efficient catalyst for tandem Knoevenagel-Michael reaction of 3-methyl-1-phenyl-1*H*-pyrazol-5(4*H*)-one with aldehydes. *Appl. Catal., A* **2013**, *467*, 61−68.
(49) Sepehrmansourie, H.; Zarei, M.; Taghavi, R.; Zolfigol, M. A. Mesoporous ionically tagged cross-linked poly (vinyl imidazole) s as novel and reusable catalysts for the preparation of *N*-heterocycle spiropyrans. *ACS Omega* **2019**, *4*, 17379−17392.

https://doi.org/10.1021/acsomega.2c06651
ACS Omega 2023, 8, 18479−18490